Clinical Neurophysiology 130 (2019) 1611–1619

Contents lists available at ScienceDirect

Clinical Neurophysiology

journal homepage: www.elsevier.com/locate/clinph

A network approach to investigate the bi-hemispheric synchrony in absence epilepsy

Pauly Ossenblok [a,b,*], Petra van Houdt [b], Albert Colon [b], Hans Stroink [c], Gilles van Luijtelaar [d]

[a] Department of Mathematics & Computer Science, Eindhoven University of Technology, Eindhoven, The Netherlands
[b] Academic Center for Epileptology Kempenhaeghe & Maastricht University Medical Center, Heeze, The Netherlands
[c] Department of Neurology, Canisius Wilhelmina Hospital, Nijmegen, The Netherlands
[d] Biological Psychology, Donders Centre of Cognition, Radboud University, Nijmegen, The Netherlands

ARTICLE INFO

Article history:
Accepted 22 May 2019
Available online 1 July 2019

Keywords:
Childhood absence epilepsy
Local connectivity mapping
Driving sources
Treatment response

HIGHLIGHTS

- A driving source initiates a cascade of events leading to the generalization of the spike-and-wave discharges (SWDs).
- Similar spatiotemporal patterns indicate common network pathways underlying generalized SWDs.
- The location of the driving source seems to be related to differences in treatment response.

ABSTRACT

Objective: Our objective was to unravel the dynamics underlying spike-and-wave discharges (SWDs) characteristic for childhood absence epilepsy.
Methods: SWDs were recorded for a cohort of 28 children using magnetoencephalography. Non-linear association analyses and a graph theoretical metric of local connectedness (LoC) were utilized in a sliding window starting one s before till four s after ictal onset.
Results: A focal pattern of bilateral frontal and parietal areas with high LoC during the spikes alternated by generalized patterns during the waves was found for all children studied during generalization of the SWDs. In the interval preceding the generalization a focal parietal region was most often (16/28) encountered and less often an occipital (4/28), temporal (5/28) or frontal (3/28) region. 55% of the children with a parietal/occipital focal onset became seizure free after the administration of two anti-epileptic drugs, and only 12.5% with a temporal/frontal focal onset.
Conclusions: The transition from the interictal to the ictal state is for some of the children characterized by dominant LoC at either the parietal/occipital and for others at the frontal/temporal region.
Significance: The focal onset of the SWDs varies in location among the children with a clinical similar profile, who, however, seemingly are differing with regard to seizure control.

1. Introduction

Absence seizures associated with bilaterally synchronized 3 Hz spike-and-wave discharges (SWDs) are prevalent in a form of genetic generalized epilepsy (Berg et al., 2010), referred to as childhood absence epilepsy (CAE). Early studies questioned based on the feline generalized penicillin epilepsy animal model whether SWDs are focal at onset or generalized and whether their origin is cortical or thalamic (e.g. Avoli and Gloor, 1982; Kostopoulos et al., 1982). Later studies in genetic rat models of CAE, provided experimental evidence that implicated a cortical onset zone in the deep layers of the somatosensory cortex followed by cortico-thalamo-cortical network interactions to maintain the SWDs (Meeren et al., 2002; Polack et al., 2007; Lüttjohann and van Luijtelaar, 2015).

Abbreviations: SWDs, spike-and-wave discharges; CAE, childhood absence epilepsy; LoC, local connectedness; MEG, magnetoencephalography; EEG-fMRI, EEG-correlated functional MRI.

* Corresponding author at: Stichting Epilepsie Instellingen Nederland (SEIN), Department of Clinical Neurophysiology, Dokter Denekampweg 20, 8025 BV Zwolle, The Netherlands.
E-mail address: possenblok@sein.nl (P. Ossenblok).

https://doi.org/10.1016/j.clinph.2019.05.034
1388-2457/

Neuroimaging studies confirmed the importance of the cortico-thalamo-cortical structures interconnected in a network in human absence epilepsy. EEG-correlated functional MRI (EEG-fMRI) studies identified a common network of structures involved in SWDs, including anterior and posterior cortices, the thalamus and the caudate nuclei, cerebellum and the reticular structures in the pons (Salek-Haddadi et al., 2003; Gotman et al., 2005; Moeller et al., 2008; Tyvaert et al., 2009). A positive BOLD response of the thalamus was initially seen as the driving source of the SWDs (Salek-Haddadi et al., 2003), however, more recently most of the studies on human absence epilepsy reported on involvement of the cortex (Seneviratne et al., 2014). While the seat of paroxysmal activity is the cortex, its emergence is only possible through thalamic interactions (Steriade and Llinás, 1988), which is in agreement with the 'cortical focus theory' based on the rat studies (Meeren et al., 2002; Polack et al., 2007). However, the location of the cortical onset area of the 3 Hz SWDs is still under debate and might be different in humans compared to rats. Carney et al. (2010) proposed that modifications in the parietal part of the default mode network drives the SWDs, while others, like Moeller et al. (2010) showed that BOLD changes in the frontal lobes became apparent during seizure onset. However, the neural network interactions at the transition from the interictal to ictal stage is likely abrupt (Suffczynski et al., 2004) and, therefore, difficult to visualize with fMRI, which may explain, together with the small and inhomogeneous sample size of most of the studies, the huge variation in the structures reported to be involved in the initiation of SWDs.

Nonlinear association analysis was used to assess the spatiotemporal dynamics of the SWDs recorded with magnetoencephalography (MEG) (Westmijse et al, 2009; Gupta et al., 2011). This method takes into account the strong nonlinear component during the transition from the interictal to the ictal state. The outcome of these studies supported the existence of significant (compared to interictal or baseline) preferred cortical areas with an alternating pattern between cortical localized and generalized activity during the evolvement of the SWDs. Moreover, the dynamic imaging procedures applied by Gupta et al. (2011) demonstrated that SWDs are not suddenly arising but gradually build up in a dynamic network, revealing a driving source of the SWDs. The aim of the current study is to describe the spatial and temporal profiles of the networks involved during the SWDs and of the driving sources initiating these discharges for a cohort of children diagnosed with CAE ($n = 28$). In addition to nonlinear association analysis, a graph theoretical metric, the local connectedness (LoC) parameter, was utilized to quantify the spatiotemporal dynamics from the interictal to the ictal state. Furthermore, it was investigated whether the spatiotemporal patterns of high LoC before ictal onset, the so called driving sources of the SWDs, differ between the children included and whether these differences are related to seizure freedom obtained during follow-up after the administration of maximally two distinct anti-epileptic drugs (AEDs).

2. Materials and methods

2.1. Patients

Twenty-eight patients were included diagnosed with CAE based on electro-clinical examinations. The inclusion criteria were in accordance with the criteria for CAE of the International League Against Epilepsy (ILAE) and similar to these utilized in the studies of Westmijse et al. (2009) and Gupta et al. (2011). After approval of this study by the Committee for Research in Humans of the region Arnhem/Nijmegen (Netherlands), written informed consent for the recordings was obtained from the parents of the children.

For all patients clinical information provided by the referring neurologists was collected prior to their participation in this study, including medical history, the use of AEDs, seizure semiology and EEG monitoring results for diagnostic purposes. The anatomical MRIs, collected either prior to the participation of the children in this study or made for the purpose of this study, did not show visible abnormalities for any of the children included in this study. The mean age of the children at the time of measurement was 8,4 years (range: 6,5–12 years) and the range of seizure onset (rounded off at 0.5) was 1.5 to 10 years, with a mean onset age of 5,7 years. The individual patient characteristics are listed in Table 1 (columns 1–3).

2.2. MEG recordings

The MEG measurements were performed with the whole head system (CTF Systems Inc., VSM MedTech Ltd., Coquitlam, BC, Canada) either at the Donders Center for Cognitive Neuroimaging at Radboud University or at VU Medical Center in Amsterdam, Netherlands. Data acquisition was identical to that described by Westmijse et al. (2009) and Gupta et al. (2011). The number of seizures recorded during measurement varied among the patients from 1 to 15, with an average of 6,2 seizures during 45 to 60 min of measurement. The bilateral synchronous SWDs were preceded by early spiking, indicated in Fig. 1 (upper row) as the visible ictal onset of the SWDs. However, for SWDs recorded during hyperventilation, issued to provoke seizures, bilateral, sometimes sharply contoured slow waves in the delta frequency range may become immediately apparent (Ossenblok et al., 2013), probably because of the effect of so called hyposynchronous slowing (HVHS) (Epstein et al., 1994; Sadleir et al., 2006). Therefore, the SWDs recorded during hyperventilation were not taken into account. Furthermore, SWDs of children with absence epilepsy become fragmented and disorganized during sleep (Sadleir et al., 2006; Sato et al., 1973) and were, therefore, also excluded. For each patient we included one of the SWDs in the analysis, which was recorded during the measurement epochs without provocation of seizure activity and without further drawbacks as artifacts due to movements during the recordings.

2.3. MEG analysis

The analysis is aimed to ascertain the existence of significant (compared to baseline) nonlinear interactions between various cortical areas of the brain across time. A nonlinear correlation analysis was utilized, as introduced by Lopes da Silva et al. (1989) and as used in our earlier studies for the same type of MEG data (Westmijse et al., 2009; Gupta et al., 2011). A network approach is followed with the MEG sensors as nodes of the network and their connections expressed by the nonlinear correlation values yielding together the functional connectivity maps. In Fig. 1 an example is shown of SWDs recorded with MEG and an illustration of the analysis procedure. Plotted is the MEG signal for the time window of analysis used with a duration of 5 sec (upper row). The analysis started 1 s before the visible onset of the SWDs, as identified and marked by an independent clinical neurophysiologist and as illustrated in Fig. 1 with a red arrow. This 1 s period is per definition the preictal period. The nonlinear correlation analysis was performed for overlapping 20 ms shifted windows of, respectively, 180 and 187.5 ms, depending on the sample frequency (either 1200 or 1250 ms) of the MEG signals (Westmijse et al., 2009), yielding for each window k and for each pair of MEG sensors (i,j) a maximal association value h^2ij (k). In Fig. 1 (middle row) the signals are shown after computation of the nonlinear correlation strength between each combination of the MEG signals shown in the upper row. The correlation strengths determine the connections between

Table 1
Patient characteristics and location of the driving sources of their SWDs.

Patient	Sex/age	Age seizure onset	Automatism? (Y/N)	Drug naïve? (Y/N)	Seizure free? (AED1,AED2)	Preictal focal area
Pat 1	M/8	6	N	N	N (CBZ,LTG)	RP
Pat 2	F/12	5	N	N	N (VPA, ESM)	LO
Pat 3	M/7.9	5	N	N	Y(LTG,Ethy)	LO
Pat 4	F/8.5	5	N	N	N(VPA,LTG)	LT
Pat 5	F/10.3	5	During HV arm/leg movement		Y(LTG, ESM)	LP
Pat 6	F/8.5	7	blinking	N	Y(VPA,ESM	RP
Pat 7	M/9	9	N	Y	Y(VPA)	RP
Pat 8	F/7	2	Smacking/swallowing/eye turning to left	N	N(VPA,ESM	LF
Pat 9	F/8.5	1.5	N	N	N(ESM,LTG)	LO
Pat 10	F/11	2.5	N	N	N(VPA,ESM)	RP
Pat 11	F/7.8	5	Eye movements/bilateral movements	N	N(LEV,ESM	LP
Pat 12	F/6.3	2	?	N	N(VPA,LTG	RP
Pat 13	M/10	2	Whole body clonias and urine loss	N	N(VPA,LEV)	RF
Pat 14	M/8.5	7	?	N	N(VPA,CBZ)	RT
Pat 15	F/8.5	6	N	N	N(VPA,LTG)	LT
Pat 16	F/7.1	6	smacking	Y	N(VPA,Ethy	LP
Pat 17	M/11.1	9	Swallowing/blinking	Y	Y(VPA)	LP
Pat 18	F/7.3	6	Arm movements	N	Y(VPA,LTG)	RO
Pat 19	M/7.6	7	Leg movements	Y	Y(VPA)	RP
Pat 20	F/8.5	7	blinking	Y	N(VPA,LEV)	RT
Pat 21	F/9.9	8	Minor myoclonias/Clapping	Y	Y(VPA)	LP
Pat 22	M/6.5	4	Urine loss	N	N(VPA,ESM)	RP
Pat 23	F/6.7	5	Eye deviations	N	N(VPA,ESM)	RP
Pat 24	M/8.8	8	Eye deviations/blinking	Y	Y(ESM,VPA)	LP
Pat 25	M/7	3	Minor clonias	N	N(VPA,ESM)	RF
Pat 26	F/8	8	N	Y	Y(ESM)	LP
Pat 27	M/7	4	Turning of the eyes	Y	Y(ESM,VPA)	LP
Pat 28	F/9	9	N	Y	Y(Ethy,VPA	LT

Listed for the 28 patients studied (Pat 1- Pat 28), are the patient characteristics, age of seizure onset, whether the patient had automatisms during the seizures, was drug naïve at the time of measurement and was seizure free after the administration of two AEDs [CBZ = Carbamazepine; Ethy = Ethymal; ESM = Ethosuximide; LMT = Lamictal; LEV = Levetiracetam; LTG = Lamotrigine; VPA = Valproat;]. In the last column is the area indicated at the lobe level [F = frontal, T = temporal, P = parietal, O = occipital] with high LoC of the MEG signals at either the right [=R] or left [=L] hemisphere. [HV = hyperventilation; N = No; Y = Yes].

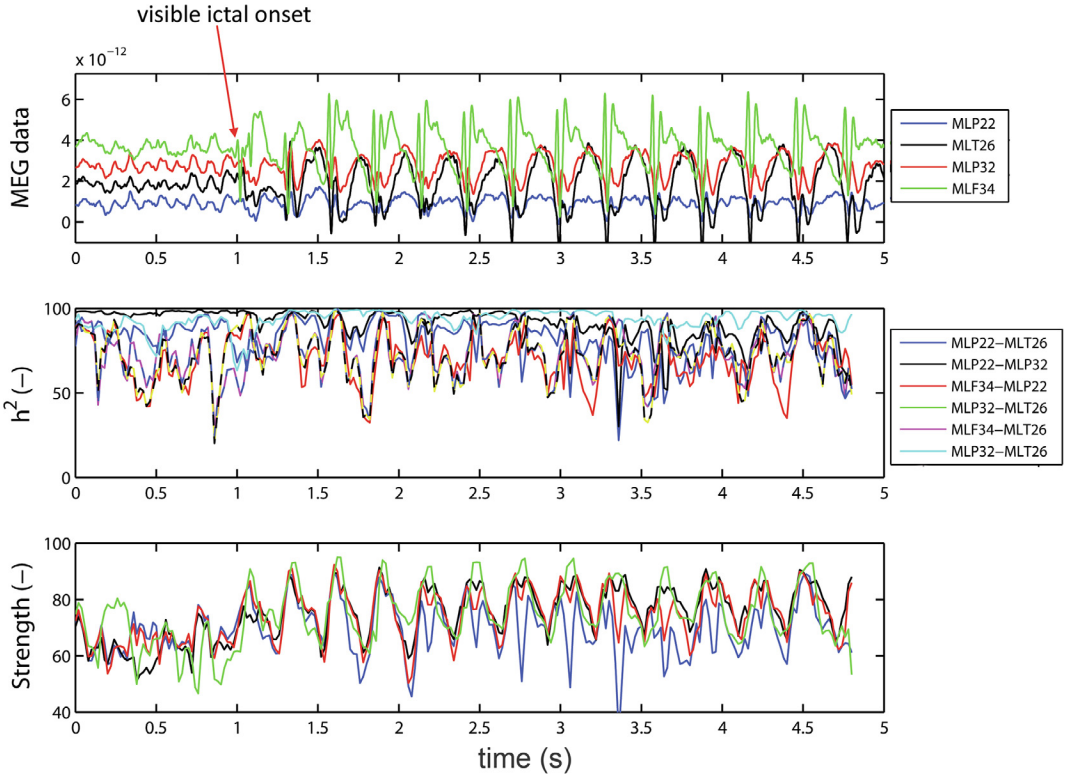

Fig. 1. The upper row shows MEG signals (in femto (10–12) Tesla) of four selected MEG (M) sensors (recorded in the left (L) parietal (P), temporal (T) and frontal (F) regions) from 1 s before the visible ictal onset (indicated by the red arrow) till 4 s after the onset of a SWD. The middle row shows the nonlinear association values (h^2), estimated for each combination of MEG sensors and each analysis window. The association strength (strength), representing the average association strength of that MEG sensor relative to the other sensors per analysis window, is presented at the bottom row.

the nodes of the network. Both Westmijse et al. (2009) as well as Gupta et al. (2011) showed that a threshold of 95% of the association strength values sets apart the interictal from ictal states. Therefore this threshold value was used again. Next, an average value was computed for each sensor, called the association strength, representing the association strength of that MEG sensor relative to all other sensors. The average of the association strength signals per MEG sensor, as shown in the upper row of Fig. 1, is shown in the bottom row of this figure.

The averaged association strength function over all sensors was computed, together with the spatial distribution of the LoC parameter. The LoC parameter was obtained by calculating the clustering coefficient, defined as the mean clustering for each time window of analysis across all nodes in the network, yielding for each MEG sensor the probability that the neighboring sensors are connected (Soffer et al., 2005). The LoC parameter was computed for each of the overlapping 20 ms shifted time windows of analysis during the period starting 1 s before the visible ictal onset till 4 s after the onset. The distribution of the LoC parameter was plotted color coded as a 2-dimensional projection (nose up) of the head surface. The averaged association strength function yields together with the changing distribution of the LoC parameter obtained for each time window of analysis the spatiotemporal changes of the activity underlying the SWDs, thus reflecting the network dynamics during the evolvement of the SWDs. For the preictal period the frequency of occurrence of high LoC values was computed for each MEG sensor to identify the location of the driving source of the SWDs of the 28 patients studied. The computation of the maximal frequency of occurrence of high LoC values, further referred to as the maximal LoC pattern, is based on the outlay of the MEG sensor distribution provided by the CTF system.

2.4. Statistical analysis

A Chi^2 test was used in order to establish whether there were preferential cortical sites containing the driving source of the SWDs. Putative differences in SWD characteristics between patients with different cortical locations of the area with the maximal LoC pattern were analyzed with a two factor ANOVA, with cortical region (4 levels) and hemisphere (2 levels) as between subjects factors; in case there was no main effect of hemisphere or interaction with hemisphere, the factor "hemisphere" was no longer included. If necessary, the ANOVAs were followed by Least Squares Difference post-hoc tests. The dependent variables were: age of onset, duration of having absence epilepsy, current age, time between ictal onset and first moment of generalization, and mean and standard deviation (SD) of the amplitude of the oscillatory pattern and mean and SD of the time difference between two successive generalizations. The same dependent variables were investigated in order to answer the question whether there were differences between children who became seizure free or not. Considering that only a medium size cohort of children was included, with the risk that some of the groups were relatively small and that some tests might be underpowered, we included a measurement for effect size, Eta^2. Eta^2 is a measure of effect size, a small effect is <0.10, between 0.10 and 0.25 is a medium, and >0.40 is considered as a strong effect. Product-Moment correlation coefficients between the dependent variables were additionally calculated to see whether there were other relations among the variables than the ones we had tested with the ANOVA's. Also logistic regression analyses was used in order to investigate whether seizure control could be predicted by either clinical or SWD parameters. For the statistical analysis SPSS-V23 was used.

3. Results

We included a medium size group of twenty-eight children with absences as the only type of seizures. Sixteen out of these twenty-eight children presented themselves during their absences with symptoms as blinking, smacking and other movement related automatisms (Table 1, column 4). However, it has been reported that if automatisms are associated with absence seizures along with bilateral synchronous SWDs the epilepsy of these children can be classified as idiopathic (nowadays genetic) generalized absence epilepsy (Panayiotopoulos, 2008). Six out of the 28 children in our study had their first seizures when they were younger than the minimal age of seizure onset in case of CAE, as reported on by Duncan (1997). However, it also has been reported that typical absence seizures presenting before the age of three, although very rare, may occur (Shahar et al., 2007). Some patients had a history of subsequent use of different AEDs (#1, 2 or 3), while ten children were drug naïve at the time of measurement (Table 1, column 5). In column 6 of Table 1 it is indicated whether the patient became seizure free or not during the follow-up after the administration of maximally two different appropriately chosen AEDs, according to the information provided by the referring neurologist.

3.1. Generalized SWDs

The result of averaging the association strength functions for all possible combinations of MEG signals for patient #11 is shown in Fig. 2A (middle row). Fig. 2B shows a selection (interval of 100 ms, increasing from left to right) of the spatial distributions of the LoC parameter computed in the period from 1 s before the visible ictal onset, indicated by the blue square, till the start of the gSWD (indicated by the first red star). Note that at the ictal onset the LoC pattern still reflects focal areas of high LoC, mainly at mesiofrontal and bilateral frontal and parietal regions (Fig. 2A, upper row left). However, at a certain point the LoC pattern transits into a bilateral synchronous widespread distribution of the SWDs (Fig. 2A, upper row right). This moment is defined as the onset of the generalized SWDs (gSWDs). The association strength function reflects during the gSWDs a rhythmic pattern of peaks and troughs (Fig. 2A, middle row). These peaks and troughs are related, respectively, to epochs with a completely generalized pattern of high connectivity values during the waves of the gSWDs alternated by a pattern that reflects bilateral frontal and parietal focal regions of high LoC during the spikes of these discharges. Because of the repetitive pattern of these generalized and focal patterns during the peaks and troughs of the association strength function averaging is allowed. The result of averaging for patient #11 is shown in the bottom row of Fig. 2A, with a maximal generalization occurring during the waves of the SWDs (red asterisk), while during the epoch centered around the maximum of the spikes of the gSWDs the bilateral focal frontal and parietal areas with high LoC occur (green circle). The alternating pattern of wide spread (generalized) high connectivity values during the waves of the SWDs alternated by focal areas of high connectivity values during the spikes is a common feature which occurred for all patients and all SWDs studied.

3.2. Parameters that characterize the gSWDs

The mean peak to peak amplitude versus the mean duration of the oscillating association strength function, as established during the gSWDs of all individual patients, is shown in Fig. 3A. Note that the amplitude versus duration graph reflects a consistent cluster, indicating that the oscillation parameters during the gSWDs are in the same range, and pretty similar, for all 28 children included.

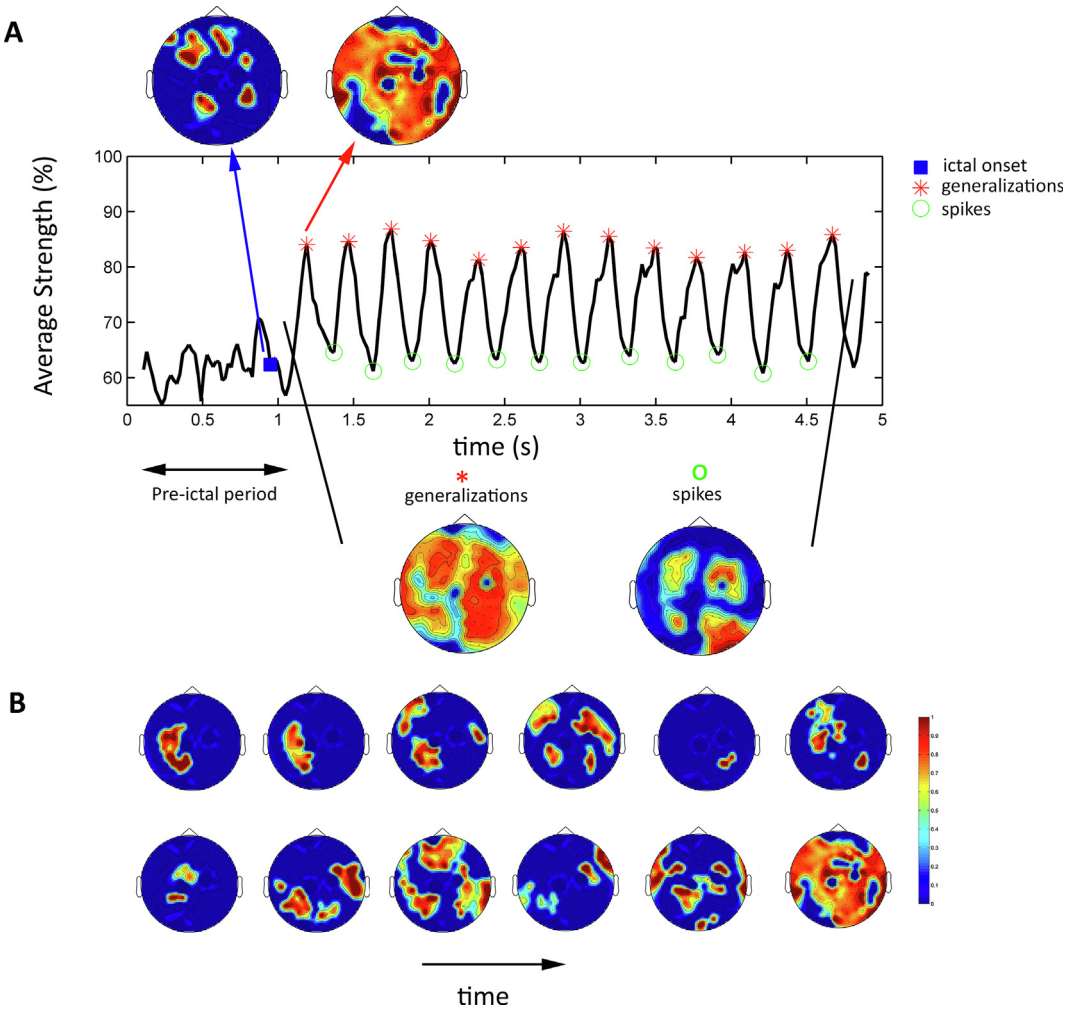

Fig. 2. A. The averaged association strength function over all sensors (in percentages) from 1 s before the ictal onset (blue square) till 4 s after the onset (middle row), is shown together with the spatial distribution of the LoC values of patient #11. Shown in the upper row (from left to right) is the distribution of LoC values computed for the epoch surrounding the visible ictal onset, which is indicated by the blue square, and for the epoch surrounding the maximal association strength during the first generalized spike-and-wave. The averaged spatial distribution of the generalized (red asterisks) and focal (green circles) patterns of high connectivity across the gSWD is shown at the bottom row. B. A selection of spatial distributions of LoC values obtained for the analysis epochs of 187.5 ms, shifted in time with 20 ms, during the epoch starting 1 s before the ictal onset till the start of the gSWDs, is shown here from left to right for subsequent analysis windows with intervals of 100 ms.

The duration of the oscillations appears to be quite consistent for all children studied, with a mean frequency of 3.1 Hz (range 2.5–3.7 Hz) across patients, which is typically for the SWDs of children with childhood absence epilepsy. Furthermore, Fig. 3B indicates that the first generalization after ictal onset plotted against the age of seizure onset occurs for the 28 patients within a period of less than 1 s, with a mean duration of 560 ms (range 234–933 ms and SD of 220 ms). This duration is in accordance with the transi-

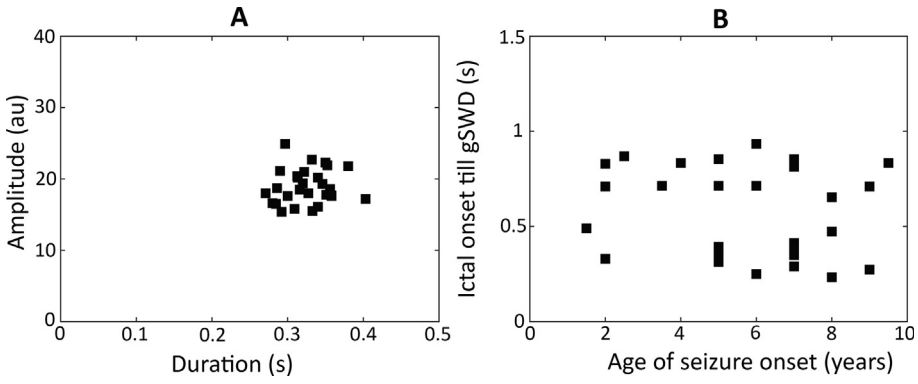

Fig. 3. A. The scatterplot of the average amplitude versus average duration of the oscillations of the SWDs for all patients included in the study yields a homogenous cluster. B. Plotted is the duration from the start of ictal activity (ictal onset), as marked by the clinical neurophysiologist, till the first generalized SWD (gSWD) versus the age of seizure onset of the patients studied.

tion period from interictal to generalized ictal activity as reported on by Gupta et al. (2011). Although, the age of seizure onset varied among the children, the time till the first generalization of the SWDs was not significantly affected by it. Furthermore, taking anti-epileptic medication during the MEG measurements did neither affect the oscillation patterns nor the time from ictal onset till the first generalization, as was established with t-tests.

3.3. Driving source of the SWDs

Focal areas of high LoC values can be observed in the period from 1 s before the visible ictal onset till the start of the gSWD (see Fig. 2B), starting with a maximum at the left parietal lobe (upper left) with a gradual build-up of other frontal and parietal areas contributing to the LoC map until the first generalization occurs (bottom right). Note that left parietal high LoC values tend to be present throughout the whole period (with a single exception), whereas the spatial distribution of the LoC values highly fluctuates across time. In Fig. 4 the computation of the maximal frequency of occurrence of high LoC values, further referred to as the maximal LoC pattern, is based on the outlay of the MEG sensor distribution provided by the CTF system.

The frequency of occurrence of high LoC values is shown in percentages for the distinct regions of the CTF-outlay of MEG sensors, as shown in Fig. 4A, for patient #11 (Fig. 4B). The most dominant contributions of the LoC parameter can be found at the left parietal (LP) MEG sensors. The maximal LoC pattern is computed for the preictal period, chosen instead of the period till the occurrence of the first generalized pattern in order to avoid a bias as result of the sudden occurrence of a completely generalized LoC pattern, as can be seen in Fig. 2B (bottom row right). The maximal LoC pattern is plotted color coded in Fig. 4C as a 2-dimensional projection of the MEG sensor outlay. The blue encircled region indicates the region with the maximal LoC pattern, from left to right for patient

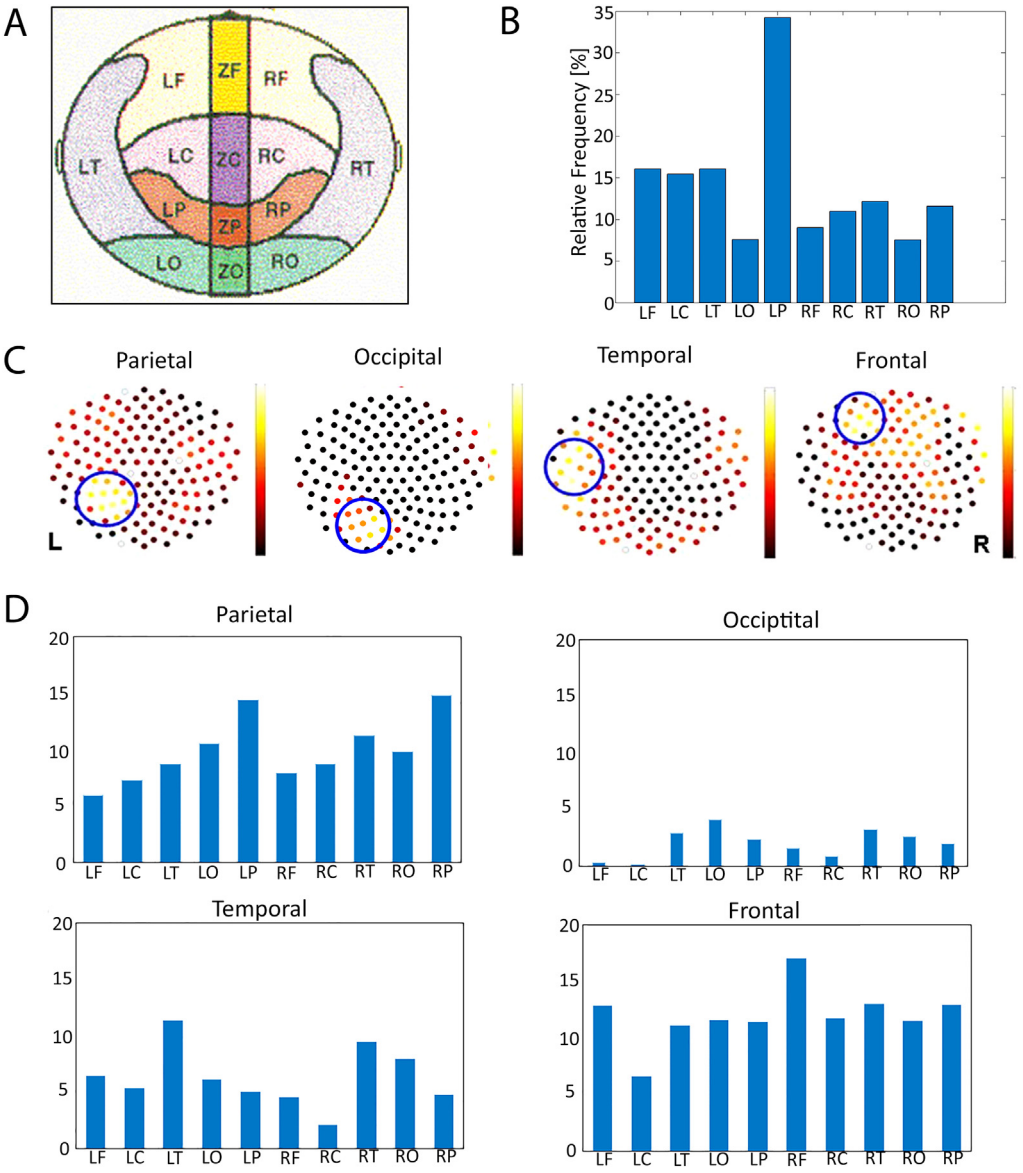

Fig. 4. A. The MEG sensor outlay of the CTF-system. B. The histogram of the relative frequency of occurrence of high LoC values (in percentages) for the distinct regions of the MEG sensor outlay [L = left; R = right, F = frontal; C = central; T = temporal; O = occipital; P = parietal] for patient #11. C. The frequency distributions of high LoC values plotted as a 2-dimensional projection of the MEG sensor outlay, with from left to right a maximal LoC pattern (indicated by the blue circle) in the parietal region for #11, in the occipital region for # 2, in the temporal region for #15 and in the frontal region for #8. D. The histograms of the relative frequency (in percentages) averaged for all patients with either a parietal, occipital, temporal or frontal maximal LoC pattern.

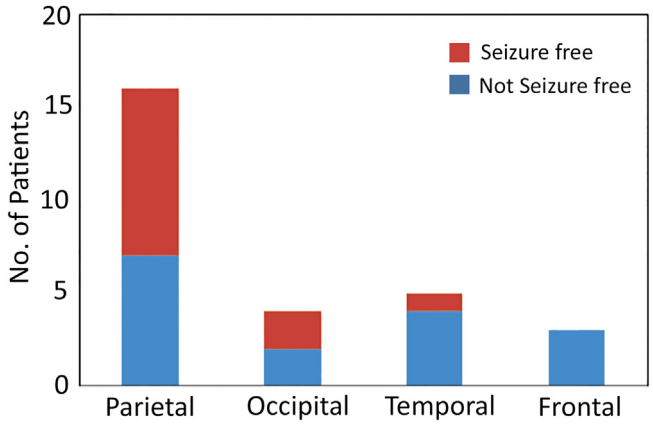

Fig. 5. Number of patients with a maximal LoC pattern, respectively, at the parietal, occipital, temporal or frontal lobe, who became seizure free (brown) or not (blue).

#11 at the left parietal region, for patient #2 at the left occipital region, for patient #15 at the left temporal region and for patient #8 at the left frontal region. Table 1 (column 7) lists the regions with the maximal LoC pattern for all the patients studied: these regions are supposed to contain the driving source of the SWDs. The result of the computations resulted in a driving source of the SWDs localized 16 times in the parietal, 4 in the occipital and 5 times in the temporal region and 3 times with a clearly frontal maximum. A Chi^2 test revealed that the hypothesis that the driving source of the SWDs has equal probabilities to be present in the different regions among the 28 patients should be rejected ($Chi^2 = 15.7$, df 3, $p < 0.001$), suggesting that the parietal cortex indeed has a higher chance to contain the driving source.

The histograms in Fig. 4D indicate the occurrence of high LoC values per region, as defined by the outlay of the CTF-system, averaged for all patients with either a parietal, occipital, temporal or frontal maximal LoC pattern. A three way ANOVA was used with patient group as in between and brain region and hemisphere as intra-subject factors, respectively, indicating that the parietal and temporal regions dominate with regard to high LoC values and that there are no differences between the two hemispheres.

In Fig. 5 the regions with the maximal LoC pattern as listed in Table 1 (column 7) are related to seizure freedom or not after the administration of maximally two AEDs, as specified in Table 1 (column 6). Note, that half of the children with a parietal or occipital dominance became seizure free, whereas only 1 out of 5 children with a maximal LoC pattern at the temporal lobe became seizure free and none of the children with a maximum at the frontal lobe. Statistical analysis indicated that only one clinical parameter was significantly related to seizure control: the age of seizure onset of children with successful seizure control was higher than of children who were not seizure free ($F = 17.01$, df 1,25, $p < 0.001$, eta2 = 0.41), suggesting a large effect size. When the group of children with either a parietal and occipital or a temporal and frontal driving source are taken together then these two groups tend to differ significantly in response to treatment as was revealed by a Chi2 test ($p < 0.06$, with a moderate effect size). Therefore, despite the limited population with a frontal/temporal driving source the results of the statistical analysis suggest that this group of children tends to be less responsive to AED treatment.

4. Discussion

A medium size group of children, who were clinically diagnosed with CAE, were studied using MEG. Network analysis of the 3 Hz SWDs, which are the hallmark of this type of epilepsy, indicated that for each of the patients studied a focal driving source can be identified, which may differ in location among the patients studied. The driving source initiates in the transition period from interictal to ictal a cascade of spatiotemporal changes resulting in the gSWDs. These gSWDs are characterized by being identical across all patients and consist of patterns of local high connectivity during the spikes and global high connectivity during the waves, irrespective of the location of the driving source of the SWDs.

4.1. Cortical driving source

Many of the studies on human generalized epilepsy support the involvement of frontal cortical areas before thalamic activation, like early depth EEG studies (Niedermeyer et al., 1969; Bancaud et al., 1974), some of the EEG-fMRI studies (Moeller et al., 2010; Bai et al., 2010; Berman et al., 2010; Szaflarski et al., 2010) and source mapping studies using either EEG (Rodin et al., 1994) or MEG (Westmijse et al., 2009). Gupta et al. (2011) showed that in case of CAE the SWDs are not suddenly arising but gradually build up in a dynamic network, with parietal/occipital cortical involvement before ictal onset, and subsequent propagation towards the frontal areas. This finding is in agreement with a study of cortical layers, by Sysoeva et al. (2016), who reported early coupling changes occurring 2 sec prior to ictal onset of the SWDs in WAG/Rij rats. The dynamics of the SWDs were studied both by Sarrigiannis et al. (2018), who used connectivity analysis based on synchronized surface EEG recordings, and Wu et al. (2017) who applied connectivity analysis on virtual sensors for distinct frequency bands. However, both groups used time windows of analysis of 1 s to localize the dominant activity during the transition from the interictal to ictal state. It is inherent for EEG-fMRI studies that time windows of analysis of at least 3 s are needed, despite time course analysis as applied in the study of Benuzzi et al. (2012). Furthermore, each of these studies presented their results on the group level and reported a mix of parietal and frontal focal initiation sites of the SWDs. The exception was the study of Sarrigiannis et al. (2018): these authors reported on a strong involvement of the central areas, which probably is a bias, because they applied their analysis on a bipolar montage of 10/20 EEG channel activity. The main difference of all of these studies with our study is the time resolution: we used time windows of less than 200 ms shifting in time with 20 ms. This enabled us to study the dynamics during the transition from interictal to ictal on the patient level in larger temporal detail. We could differentiate between children with a maximal LoC pattern in the parietal regions (16 out of 28; see Table 1, last column), while a minority showed the maximal LoC pattern at either the occipital, temporal or frontal lobe. A parietal driving source of the SWDs is in line with earlier reports by e.g. Carney et al. (2010) and by Vaudano et al. (2009), who demonstrated that bilateral haemodynamic changes in the precuneus had an active role in the initiation of the gSWDs. Interestingly, the overall contribution of the occipital region to the LoC pattern is clearly less dominant (see Fig. 4D) compared to, especially, the parietal and frontal region. Therefore, it can be concluded that the amount of connectivity during the preictal period is highest in the parietal and frontal cortex and the lowest in the occipital cortex. New is that the driving sources, as expressed by the focal LoC pattern, do not seem to be static, but express itself as a spatial dynamic collective of focal areas including the bilateral frontal and parietal areas, which are also activated for each patient during the generalization of the SWDs (see Fig. 2). Thus, the results presented provide evidence for a dynamic bilateral cortical network underlying the transition from the interictal to ictal state of the SWDs. However, despite the high variability in these LoC patterns during the transition, we were able to differentiate between

children with dominant connectivity at either the parietal/occipital or the frontal/temporal areas (see also Fig. 4D). These results are in line with the findings of a recent study of Tenney et al. (2018), who used EEG-fMRI informed MEG connectivity analysis indicating that the parietal versus frontal dominance can be explained by the activity of two distinct dynamic networks during the transition from interictal to ictal. The involvement of dynamic networks during the initiation of the SWDs also might explain that there is sometimes a left sided onset and sometimes a right sided onset of the SWDs in the same child, as was reported on by Gupta et al. (2011) and as observed for the children included in this study.

4.2. Common pathway during generalization

We showed that the repetitive pattern of bilateral synchronous generalized activity during the waves and bilateral focal frontal and parietal areas during the spikes (see Fig. 2A) is the most stable characteristic of SWDs occurring in the MEG of children with absence epilepsy, irrespective of the location of the driving source of the SWDs. Also the findings of Youssofzadeh et al. (2018) are in support of our finding that a transition takes place from highly connected brain areas till the occurrence of the rhythmic pattern of large-scale generalization during the waves of the SWDs. The results presented indicate that a common network is activated, with an intact cortico-thalamo-cortical circuit which is imperative for the rhytmogenesis (Avoli et al., 2012) and with bilateral cortical involvement, which was confirmed by beamformer analysis of the spikes occurring bilateral during the gSWDs (Westmijse et al., 2009).

4.3. Clinical implications

The signal analysis methods developed in this study to identify the driving source of the SWDs appear to be useful to differentiate to some extent between children with absence epilepsy who may respond to initial AED treatment, i.e. those with a parietal and occipital driving source, while others tend to be less responsive, mainly the children with a temporal or frontal location of the driving source (see Fig. 5). It has been reported that seizures of children with frontal absence epilepsy are refractory, persist and may go with severe cognitive impairments (Lagae et al., 2001), while the SWDs of patients who develop even more severe types of seizures are associated with activation of medial frontal and orbital frontal cortices (Holmes et al., 2004). Further support for our results was provided recently by Tenney et al. (2018) who reported that non-responders to ethosuximide treatment had decreased pretreatment cortical connectivity in the precuneus and increased in the frontal regions compared to responders. Apparently, differences in connectivity are related to the variable treatment response seen in patients sharing the same clinical epilepsy syndrome. Knowledge about the location of the driving source of the SWDs may help the clinician to understand why children with a similar clinical profile differ in treatment response, and why some may find relief by alternative treatment strategies. On the other hand, understanding the dynamics during the transition from interictal to ictal may prevent misdiagnosis as focal epilepsy and as a consequence delayed diagnosis of genetic generalized epilepsy. Clinicians need, according to Seneviratne and coworkers (2014), be aware of this pitfall.

Most of the recent studies on CAE agree on a focal cortical onset of generalized SWDs and many doubt whether there is such a thing as "generalized" epilepsy (Holmes et al., 2004; van Luijtelaar et al., 2014; Scicchitano et al., 2015). The bilateral frontal and parietal hubs (see Fig. 2), which become apparent during the spikes of the SWDs and remain stable throughout the whole gSWD, as was confirmed with beamformer analysis (Westmijse et al., 2009), represent most likely a cortical network involved during the entire SWDs. It can only be speculated that these cortical hubs are part of the default network, fitting in line with a network hypotheses of generalized genetic epilepsies (Stefan et al., 2013). Considering the differences in location of the driving source, it is not likely that the network that initiates a generalized seizure is identical to the network involved in generalization, maintenance and ending of SWDs. The view that absence epilepsy is governed by several coupled networks has obviously consequences when considering surgical treatment options.

4.4. Limitations of the study

Both MEG and EEG-fMRI studies indicated the involvement of parietal and frontal regions in the initiation of SWDs. The importance of other cortical regions obtained with fMRI like the precuneus, and subcortical regions as the caudate nucleus and the thalamus during absence seizures could not be confirmed with MEG only, because MEG is less sensitive for sources originating in the deeper (thalamic) brain structures due to the inferior signal-to-noise ratio of MEG compared to EEG in these structures (de Jongh et al., 2005; Goldenholz et al., 2009). Note, however, that fMRI-informed MEG connectivity analysis applied by Tenney et al. (2018) identified, apart from cortical areas, also thalamic sources. A further limitation of our study is that we applied association analysis on surface MEG recordings, which reflects mixed involvement of distinct cortical sources. However, beamformer analysis (Gross et al., 2001; Robinson et al., 2004) also indicated significant activations underlying the spikes of the SWDs in bilateral frontal and parietal areas (Westmijse et al., 2009; Gupta et al., 2011). Moreover, in the study of Wu et al. (2017) similar analysis procedures applied to virtual source signals yielded similar conclusions.

5. Conclusions

Our analysis approach enabled us to study in detail the dynamics on the patient level during the transition from the interictal to ictal state and the subsequent transition to a stable common pathway pattern during the gSWDs, which appeared to be similar for all children studied. The high temporal and spatial distribution network analysis revealed focal network activity during the spikes of the SWDs and global network activity during the waves of the gSWDs. A cortical driving source initiates these gSWDs, which differs in location, despite a similar clinical epilepsy syndrome of the children studied. Differentiation in location of these driving sources may have clinical relevance, because of its relation to the responsiveness to AED treatment. However, we have to be aware that the number of children included is restricted, and the subdivision into several subgroups brings restrictions concerning whether and if the results, as reported here, translate to a larger population.

Declaration of Competing Interest

None of the authors have potential conflicts of interest to be disclosed.

Acknowledgements

This study was partly funded by the Netherlands Organization for Scientific

Research (NWO), grant number 400-04-483 to GvL and PO and partly by the Dutch innovation funds of health insurers. We would like to thank Prof. Dr. P. Fries and Prof. Dr. O. Jensen for providing hospitality at the Donders center for NeuroImaging and Prof. C. Stam and Dr. A. Hillebrand for hosting the study at VU Medical

Center Amsterdam. The children were referred for the MEG study by neurologists of the Academic Center for Epileptology, Kempenhaeghe, Canisius Wilhelmina Hospital Nijmegen, University Medical Center Utrecht and TerGooi Hospital Blaricum (The Netherlands). The authors thank, especially, the Academic Center of Epileptology, Kempenhaeghe for the contribution to the data collection and review.

References

Avoli M. A brief history on the oscillating roles of thalamus and cortex in absence seizures. Epilepsia 2012;53:779–89.
Avoli M, Gloor P. Interaction of cortex and thalamus in spike and wave discharges of feline generalized penicillin epilepsy. Exp Neurol 1982;76:196–217.
Bai X, Vestal M, Berman R, Negishi M, Spann M, Vega C, et al. Dynamic time course of typical childhood absence seizures: EEG, behavior, and functional magnetic resonance imaging. J Neurosci 2010;30:5884–93.
Bancaud J, Talairach J, Morel P, Bresson M, Bonis A, Geier S, et al. "Generalized" epileptic seizures elicited by electrical stimulation of the frontal lobe in man. Electroencephalogr Clin Neurophysiol 1974;37:275–82.
Benuzzi F, Mirandola L, Pugnaghi M, Farinelli V, Tassinari CA, Capovilla G, et al. Increased cortical BOLD signal anticipates generalized spike and wave discharges in adolescents and adults with idiopathic generalized epilepsies. Epilepsia 2012;53:622–30.
Berg AT, Berkovic SF, Brodie MJ, Buchhalter J, Cross JH, van Emde Boas W, et al. Revised terminology and concepts for organization of seizures and epilepsies: report of the ILAE Commission on Classification and Terminology, 2005–2009. Epilepsia 2010;51:676–85.
Berman R, Negishi M, Vestal M, Spann M, Chung MH, Bai X, et al. Simultaneous EEG, fMRI, and behavior in typical childhood absence seizures. Epilepsia 2010;51:2011–22.
Carney PW, Masterton RA, Harvey AS, Scheffer IE, Berkovic SF, Jackson GD. The core network in absence epilepsy. Differences in cortical and thalamic BOLD response. Neurology 2010;75:904–11.
de Jongh A, de Munck JC, Gonçalves SI, Ossenblok P. Differences in MEG/EEG epileptic spike yields explained by regional differences in signal-to-noise ratios. J Clin Neurophysiol 2005;22:153–8.
Duncan JS. Idiopathic generalized epilepsies with typical absences. J Neurol 1997;244:403–11.
Shahar E, Kramer U, Mahajnah M, Lerman-Sagie T, Goez R, Gross V, et al. Typical absence epilepsy presenting prior to age of 3 years: An uncommon form of idiopathic generalized epilepsy. Eur J Paediatric Neur 2007;1:346–52.
Epstein MA, Duchowny M, Jayakar P, Resnick TJ, Alvarez LA. Altered responsiveness during hyperventilation-induced EEG slowing: a non-epileptic phenomenon in normal children. Epilepsia 1994;35:1204–7.
Goldenholz DM, Ahlfors SP, Hämäläinen MS, Sharon D, Ishitobi M, Vaina LM, et al. Mapping the signal-to-noise-ratios of cortical sources in magnetoencephalography and electroencephalography. Hum Brain Mapp 2009;30:1077–86.
Gotman J, Grova C, Bagshaw A, Kobayashi E, Aghakhani Y, Dubeau F. Generalized epileptic discharges show thalamocortical activation and suspension of the default state of the brain. Proc Natl Acad Sci U S A 2005;102:15236–40.
Gross J, Kujala J, Hamalainen M, Timmermann L, Schnitzler A, Salmelin R. Dynamic imaging of coherent sources: Studying neural interactions in the human brain. Proc Natl Acad Sci U S A 2001;98:694–9.
Gupta D, Ossenblok P, van Luijtelaar G. Space-time network connectivity and cortical activations preceding spike wave discharges in human absence epilepsy: a MEG study. Med Biol Eng Comput 2011;49:555–65.
Holmes MD, Brown M, Tucker DM. Are "generalized" seizures truly generalized? Evidence of localized mesial frontal and frontopolar discharges in absence. Epilepsia 2004;45:1568–79.
Kostopoulos G, Avoli M, Pellegrini A, Gloor P. Laminar analyss of spindles and of spikes of the spike and wave discharge f feline generalized penicillin epilepsy. Electroencephalogr Clin Neurophysiol 1982;53:1–13.
Lagae L, Pauwels J, Monté CP, Verhelle B, Vervisch I. Frontal absences in children. Eur J Paediatr Neurol 2001;5:243–51.
Lopes da Silva F, Pijn P, Boeijinga P. Interdependence of EEG signals: linear vs. nonlinear associations and the significance of time delays and phase shifts. Brain Topogr 1989;2:9–18.
Lüttjohann A, van Luijtelaar G. Dynamics of networks during absence seizure's on- and offset in rodents and man. Front Physiol 2015;5:6–16.
Meeren HK, Pijn JP, van Luijtelaar EL, Coenen AM, Lopes da Silva FH. Cortical focus drives widespread corticothalamic networks during spontaneous absence seizures in rats. J Neurosci 2002;22:1480–95.
Moeller F, Siebner HR, Wolff S, Muhle H, Granert O, Jansen O, et al. Simultaneous EEG-fMRI in drug-naive children with newly diagnosed absence epilepsy. Epilepsia 2008;49:1510–9.
Moeller F, LeVan P, Muhle H, Stephani U, Dubeau F, Siniatchkin M, et al. Absence seizures: individual patterns revealed by EEG-fMRI. Epilepsia 2010;51:2000–10.
Niedermeyer E, Laws Jr ER, Walker EA. Depth EEG findings in epileptics with generalized spike-wave complexes. Arch Neurol 1969;21:51–8.
Ossenblok P, van Houdt P, Lüttjohann A, van Luijtelaar G. Network analysis of generalized epileptic discharges. In: Tetzlaff R, Elger CE, Lehnertz K, editors. Proceedings of the 5th international workshop on seizure prediction. World Scientific Publishing Co; 2013. p. 197–214.
Panayiotopoulos CP. Typical absence seizures and related epileptic syndromes: assessment of current state and directions for future research. Epilepsia 2008;49:2131–9.
Polack PO, Guillemain I, Hu E, Deransart C, Depaulis A, Charpier S. Deep layer somatosensory cortical neurons initiate spike-and-wave discharges in a genetic model of absence seizures. J Neurosci 2007;27:6590–9.
Robinson SE, Nagarajan SS, Mantle M, Gibbons V, Kirsch H. Localization of interictal spikes using SAM(g2) and dipole fit. Neurol Clin Neurophysiol 2004;74:1–4.
Rodin EA, Rodin MK, Thompson JA. Source analysis of generalized spike-wave complexes. Brain Topogr 1994;7:113–9.
Sadleir LG, Farrell K, Smith S, Connolly MB, Scheffer IE. Electroclinical features of absence seizures in childhood absence epilepsy. Neurology 2006;67:413–8.
Salek-Haddadi A, Lemieux L, Merschhemke M, Friston KJ, Duncan JS, Fish DR. Functional magnetic resonance imaging of human absence seizures. Ann Neurol 2003;53:663–7.
Sarrigiannis PG, Zhao Y, He F, Billings SA, Baster K, Rittey C, et al. The cortical focus in childhood absence epilepsy; evidence from nonlinear analysis of scalp EEG recordings. Clin Neurophysiol 2018;129:602–17.
Sato S, Dreifuss F, Penry J. The effect of sleep on spike-wave discharges in absence seizures. Neurology 1973;23:1335–45.
Scicchitano F, van Rijn CM, van Luijtelaar G. Unilateral and bilateral cortical resection: effects on spike-wave discharges in a genetic absence epilepsy model. PLoS ONE 2015;10(8). e0133594.
Seneviratne U, Cook M, D'Souza W. Focal abnormalities in idiopathic generalized epilepsy: a critical review of the literature. Epilepsia 2014;55:1157–69.
Soffer SN, Vázquez A. Network clustering coefficient without degree-correlation biases. Phys Rev E Stat Nonlin Soft Matter Phys 2005;71. 057101.
Stefan H, Lopes da Silva FH. Epileptic neuronal networks: methods of identification and clinical relevance. Front Neurol 2013;1:4–8.
Steriade M, Llinás RR. The functional states of the thalamus and the associated neuronal interplay. Physiol Rev 1988;68:649–742.
Sufficzynski P, Kalitzin S, Lopes de Silva FH. Dynamics of non-convulsive epileptic phenomena Modeled by a bistable neural network. Neuroscience 2004;126:467–84.
Sysoeva MV, Lüttjohann A, van Luijtelaar G, Sysoev IV. Dynamics of directional coupling underlying spike-wave discharges. Neuroscience 2016;314:75–89.
Szaflarski JP, DiFrancesco M, Hirschauer T, Banks C, Privitera MD, Gotman J, et al. Cortical and subcortical contributions to absence seizure onset examined with EEG/fMRI. Epilepsy Behav 2010;18:404–13.
Tenney JR, Kadis DS, Agler W, Rozhkov L, Altaye M, Xiang J, et al. Ictal connectivity in childhood absence epilepsy: Associations with outcome. Epilepsia 2018;59:971–81.
Tyvaert L, Chassagnon S, Sadikot A, LeVan P, Dubeau F, Gotman J. Thalamic nuclei activity in idiopathic generalized epilepsy: an EEG-fMRI study. Neurology 2009;73:2018–22.
van Luijtelaar G, Behr C, Avoli M. Is there such a thing as "generalized" epilepsy? Adv Exp Med Biol 2014;813:81–91.
Vaudano AE, Laufs H, Kiebel SJ, Carmichael DW, Hamandi K, Guye M, et al. Causal hierarchy within the Thalamo-cortical network in spike and wave discharges. PLoS One 2009;4(8):e6475.
Westmijse I, Ossenblok P, Gunning B, van Luijtelaar G. Onset and propagation of spike and slow wave discharges in human absence epilepsy: A MEG study. Epilepsia 2009;12:2538–48.
Wu C, Xiang J, Jiang W, Huang S, Gao Y, Tang L, et al. Altered effective connectivity network in childhood absence epilepsy: a multi-frequency MEG study. Brain Topogr 2017;30:673–84.
Youssofzadeh V, Agler W, Tenney JR, Kadis DS. Whole-brain MEG connectivity-based analyses reveals critical hubs in childhood absence epilepsy. Epilepsy Res 2018;145:102–9.